

## **Membrane accessibility of glutathione**

Alvaro Garcia<sup>a</sup>, Nasma D. Eljack<sup>a</sup>, Marc-Antoine Sani<sup>b</sup>, Frances Separovic<sup>b</sup>,  
Helge H. Rasmussen<sup>c,d</sup>, Wojciech Kopec<sup>e</sup>, Himanshu Khandelia<sup>e</sup>, Flemming  
Cornelius<sup>f</sup>, and Ronald J. Clarke<sup>a,\*</sup>

<sup>a</sup> *School of Chemistry, University of Sydney, Sydney, NSW 2006, Australia*

<sup>b</sup> *School of Chemistry, Bio21 Institute, University of Melbourne, Melbourne,  
VIC 3010, Australia*

<sup>c</sup> *Department of Cardiology, Royal North Shore Hospital, Sydney, NSW 2065,  
Australia*

<sup>d</sup> *Kolling Institute, University of Sydney, Sydney, NSW 2065, Australia*

<sup>e</sup> *Center for BioMembrane Physics, University of Southern Denmark, Odense  
M5230, Denmark*

<sup>f</sup> *Department of Biomedicine, University of Aarhus, DK-8000 Aarhus C,  
Denmark*

Address correspondence to Assoc. Prof. Ronald J. Clarke, School of Chemistry, University of Sydney, Sydney, NSW 2006, Australia. Tel.: 61-2-93514406; Fax: 61-2-93513329; E-mail: ronald.clarke@sydney.edu.au.

## **Abstract**

Regulation of the ion pumping activity of the Na<sup>+</sup>,K<sup>+</sup>-ATPase is crucial to the survival of animal cells. Recent evidence has suggested that the activity of the enzyme could be controlled by glutathionylation of cysteine residue 45 of the β-subunit. Crystal structures so far available indicate that this cysteine is in a transmembrane domain of the protein. Here we have analysed via fluorescence and NMR spectroscopy as well as molecular dynamics simulations whether glutathione is able to penetrate into the interior of a lipid membrane. No evidence for any penetration of glutathione into the membrane was found. Therefore, the most likely mechanism whereby the cysteine residue could become glutathionylated is via a loosening of the α-β subunit association, creating a hydrophilic passageway between them to allow access of glutathione to the cysteine residue. By such a mechanism, glutathionylation of the protein would be expected to anchor the modified cysteine residue in a hydrophilic environment, inhibiting further motion of the β-subunit during the enzyme's catalytic cycle and suppressing enzymatic activity, as has been experimentally observed. The results obtained, therefore, suggest a possible structural mechanism of how the Na<sup>+</sup>,K<sup>+</sup>-ATPase could be regulated by glutathione.

**Keywords:** sodium pump; regulation; glutathionylation; beta-subunit; phosphatidylcholine; plasma membrane

## 1. Introduction

Glutathione (see Fig. 1) is a tripeptide found ubiquitously in the cytoplasm of eukaryotic cells. In mammalian cells it is typically present at a concentration in the range 5 - 10 mM [1]. Apart from its traditional role as a reducing and antioxidant agent, glutathione participates in a wide variety of cellular processes, for example, xenobiotic detoxification [1] and redox-dependent intracellular signalling [2]. Because the cysteine residue has a highly reactive sulfhydryl group, glutathione has the capacity to form stable mixed disulfide bonds with a variety of cellular proteins [3]. The ease of reversibility of these reactions by the thiol-disulfide oxidoreductase superfamily of enzymes makes modifications of protein thiol groups by glutathione an excellent candidate for redox signal transduction [4].

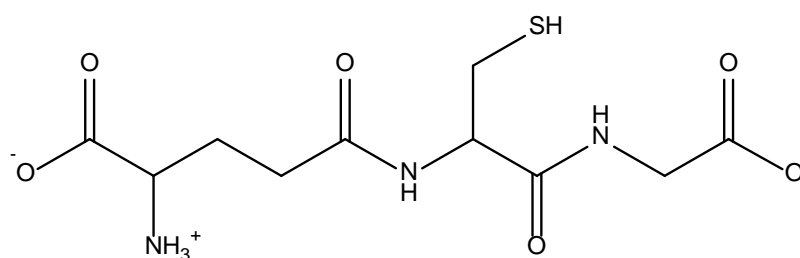


Figure 1: Chemical structure of glutathione at neutral pH.

In certain membrane proteins the target cysteine for glutathionylation resides in a cytoplasmic domain of the protein, enabling unimpeded attack by glutathione located in the cytosol [5]. However, not all susceptible cysteines reside in easily accessible areas for a charged molecule like glutathione. Cysteine 45 of the  $\beta_1$  subunit of mammalian  $\text{Na}^+, \text{K}^+$ -ATPase (or cysteine 46 in the case of the  $\beta_1$  of the shark enzyme), for example, has been reported to be susceptible to glutathionylation [6], but based on all crystal structures of the protein so far published [7-13], this cysteine is specific for the  $\beta_1$  isoform and is located within a transmembrane domain of the protein, i.e., in a region expected to have a low

polarity (see Fig. 2). Experiments have shown that an inverse relationship exists between the activity of the  $\text{Na}^+, \text{K}^+$ -ATPase and its level of glutathionylation [6, 14]. These results suggest that glutathionylation could play an important regulatory role for this enzyme and perhaps for other membrane bound proteins. Therefore, the question of how a charged hydrophilic molecule such as glutathione can access a membrane-embedded cysteine residue has mechanistic relevance for membrane protein regulation, particularly for that of the  $\text{Na}^+, \text{K}^+$ -ATPase.

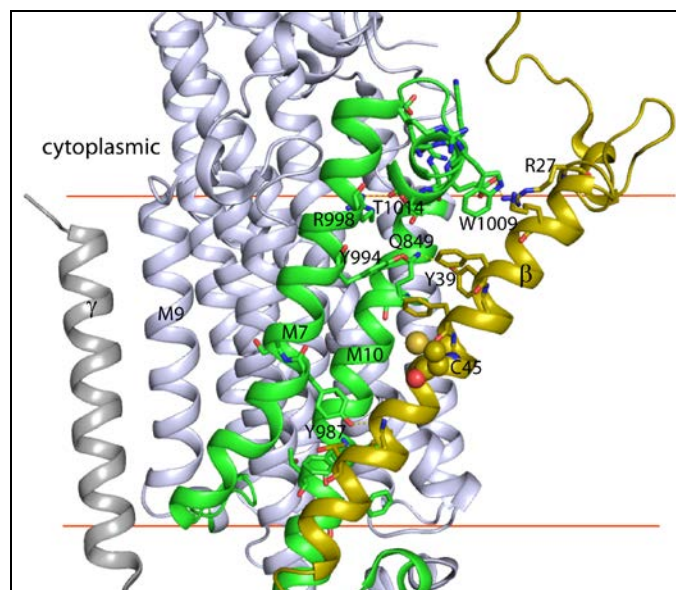


Figure 2: The transmembrane domain of pig kidney  $\text{Na}^+, \text{K}^+$ -ATPase in the  $\text{E1} \sim \text{P} \cdot \text{ADP} \cdot 3\text{Na}^+$  state (PDB ID: 3WGV). The location of Cys45 on the  $\beta$ -subunit (yellow) is shown in yellow spheres. Residues lining the interface between M7 and M10 of  $\alpha$  (green) and the  $\beta$ -subunit, forming a passageway from the cytoplasmic face of the pump to Cys45, are indicated in stick representation. R27 and Y39 on  $\beta$  are within interacting distance from W1009 and Q849, respectively, on  $\alpha$ M10. Helices of the  $\alpha$ -subunit, except M7 and M10, are in light blue, the  $\gamma$ -subunit (FXVD2) positioned alongside M9 is in grey. The approximate location of membrane borders is indicated by orange lines.

Glutathione has a net negative charge at neutral pH and is highly water soluble and, therefore, would be expected to reside in an aqueous environment. However, there is clear evidence from electrophoretic studies [15, 16] and fluorescence measurements using membrane-bound voltage-sensitive dyes [17] on lipid vesicles that some anions (e.g.  $\text{ClO}_4^-$ ,  $\text{SCN}^-$ ,  $\text{I}^-$  and  $\text{NO}_3^-$ ) are capable of binding to the membrane surface. The preference for the binding of these anions over that of small cations such as alkali metal and alkaline earth seems to be due to a combination of effects, i.e., larger size, lower hydration energies and their attraction by the positive dipole potential within phosphatidylcholine membranes. Fluorescence studies indicate that these anions decrease the dipole potential, which suggests that they are even able to penetrate below the surface of the membrane [17]. For the most strongly binding of these small anions, i.e.,  $\text{ClO}_4^-$ , reported dissociation constants are in the range 5 – 100 mM [15-17], which would generally be classed as a weak interaction, consistent with the fact that most perchlorate salts are highly water soluble. Nevertheless, these experiments have shown that anions are able to penetrate into lipid membranes and, thus, membrane penetration by glutathione cannot be *a priori* excluded. The aim of this paper is to investigate the degree to which glutathione can penetrate into a biological membrane and, thus, to examine the possibility that, under physiological conditions, glutathionylation of the relevant cysteine of the  $\beta$ -subunit of the  $\text{Na}^+, \text{K}^+$ -ATPase could occur via attack from glutathione molecules present in the lipid membrane adjacent to the protein.

## **2. Materials and methods**

### *2.1 Enzyme and reagents*

$\text{Na}^+, \text{K}^+$ -ATPase-containing open membrane fragments from pig kidney were purified as described by Klodos *et al.* [18]. The specific ATPase activity at 37°C and pH 7.4 was measured according to Ottolenghi [19] to be 2020  $\mu\text{mol ATP hydrolysed h}^{-1} (\text{mg of protein})^{-1}$

at saturating substrate concentrations. The protein concentration was  $4.98 \text{ mg mL}^{-1}$  according to the Peterson modification [20] of the Lowry method [21] using bovine serum albumin as a standard.

Dimyristoylphosphatidylcholine (DMPC) was obtained from Avanti Polar Lipids (Alabaster, AL, USA). Unilamellar vesicles were prepared by the ethanol injection method described in Zouni *et al.* [22, 23]. Dialysis tubing was purchased from Spectrum Laboratories (Rancho Dominguez, CA, USA). The DMPC concentration of the vesicle suspension was 3 mM, determined by a Phospholipid C test kit (Wako Pure Chemicals, Osaka, Japan) using a Shimadzu UV-2450 UV-visible spectrophotometer. All fluorescence measurements carried out using vesicles were performed in buffer containing 30 mM tris[hydroxymethyl]-aminomethane (Tris), 1 mM EDTA and 150 mM NaCl. The pH was adjusted to 7.2 with HCl.

4-(2-(6-(dioctylamino)-2-naphthalenyl)ethyl-1-(3-sulphopropyl)-pyridinium salt (di-8-ANEPPS) was obtained from Molecular Probes (Eugene, OR, USA) and used without further purification. 5  $\mu\text{l}$  of an ethanolic dye solution (1.0 mM) was added to 1 ml of vesicle-containing aqueous solution, so that the final solution contained 5.0  $\mu\text{M}$  of di-8-ANEPPS. The final solutions thus contained a small percentage of 0.5% ethanol. After addition of the dye, the solutions were left overnight to allow for dye disaggregation and incorporation into the membrane. The effect of the small volume of ethanol added on the fluorescence spectra of membrane-bound dye was checked in separate control measurements and found to be negligible.

The origins of the reagents used were: Tris (minimum 99.9%, Sigma); EDTA (99%, Sigma); reduced L-glutathione ( $\geq 98\%$ , Sigma); NaOH (analytical grade, Merck); KOH (analytical grade, Sigma);  $\text{MgCl}_2 \cdot 6\text{H}_2\text{O}$  ( $\geq 99\%$ , Sigma); NaF ( $\geq 99\%$ , Sigma) and HCl (0.1 N Titrisol solution, Merck).

The origins of the antibodies used were: monoclonal mouse anti-glutathione antibody (Virogen, MA, USA); anti-Na<sup>+</sup>/K<sup>+</sup>-ATPase  $\beta_1$  antibody (Merck Millipore, MA, USA); goat anti-mouse IgG (H+L) secondary antibody-horseradish peroxidase conjugate (Thermo Scientific, MA, USA) and SuperSignal West Pico Chemiluminescent Substrate (Thermo Scientific).

### *2.1 Fluorescence measurements*

Fluorescence measurements using di-8-ANEPPS were carried out with a Shimadzu (Kyoto, Japan) RF-5301 PC spectrofluorophotometer using quartz semimicro cuvettes. The fluorescence emission was measured at an emission wavelength of 670 nm. To minimize the effects of scattering of the exciting light and higher order wavelengths, an RG645 glass cut-off filter (Schott, Mainz, Germany) was used in front of the emission monochromator. The fluorescence excitation ratio,  $R$ , was measured before and after the addition of varying concentrations of glutathione to the vesicles.  $R$  is defined as the ratio of fluorescence intensity at an excitation ratio of 420 nm divided by that at 520 nm. The wavelengths were chosen based on a previous study [24] to avoid any effects of membrane fluidity on the measured fluorescence ratios. Glutathione was added from a buffer solution with the same composition as the buffer solution used for vesicle preparation. Both buffer solutions were adjusted with either HCl or NaOH to a pH of 7.2, i.e., more than 5 pH units above the apparent  $pK_a$  of membrane-bound di-8-ANEPPS of <1.9 [25]. Because of the necessity of adjusting the pH of the glutathione solution with NaOH, the addition of glutathione to the vesicles increases slightly the Na<sup>+</sup> concentration and decreases slightly the Cl<sup>-</sup> concentration of the solution. However, independent experiments [17] have shown that NaCl up to a concentration of at least 0.5 M has no effect on the fluorescence excitation spectrum of membrane-bound di-8-ANEPPS. The temperature was maintained at 30°C via a circulating water bath, i.e., above

the main phase transition temperature of DMPC of 23°C [26], so that the lipid was in its liquid crystalline state.

## 2.2 NMR measurements

Acyl chain perdeuterated DMPC ( $d_{54}$ -DMPC) was obtained from Avanti Polar Lipids (Alabaster, USA). A 130 mM GSH stock solution was made in 30 mM Tris buffer (pH 7.3, readjusted with HCl) with 150 mM NaCl and 1 mM EDTA. An appropriate volume of glutathione was added to the lipid powder in order to obtain a lipid to peptide molar ratio of 20:1 and 5:1, with a hydration level of 65% (w/w). Three freeze/thaw cycles were then performed prior to packing into a 3.2 mm NMR rotor. Experiments were run at 30°C.

$^{31}\text{P}$  static and magic angle spinning (MAS) solid-state NMR experiments were performed at 242.76 MHz on a Varian (Palo Alto, USA) 600 MHz spectrometer using a 3.2 mm HXY BioMAS probe (Varian). Static  $^{31}\text{P}$  NMR spectra were collected under 57 kHz SPINAL64 proton decoupling using a single  $\pi/2$ -pulse with duration of 4.25  $\mu\text{s}$ . A minimum of 1024 transients was acquired at a spectral width of 125 kHz and Fourier transformed following 50 Hz exponential line broadening.  $^{31}\text{P}$  relaxation experiments were carried out under MAS at 10 kHz.  $T_1$  relaxation times were measured using the inversion recovery pulse sequence. Typical recycle delays were 3 s with 15 variable  $\tau$ -delay values between 0 and 3 s.  $T_2$  relaxation times were measured with a Hahn spin-echo experiment with total echo delay ( $\tau$ ) values between 0.2 and 20 ms at integer multiples of the rotor period. The chemical shift anisotropy (CSA) and the asymmetry of the  $^{31}\text{P}$  tensor were obtained by MEMAS analysis [27].  $^{31}\text{P}$  MAS spectra were collected at 700 Hz, 900 Hz and 1200 Hz under similar conditions as used for static  $^{31}\text{P}$  experiments.

$^2\text{H}$  static NMR experiments were performed at 92.06 MHz with the same probe. A solid-echo with  $\pi/2$ -pulse duration of 5.5  $\mu\text{s}$  and a recycle delay of 0.5 s were used. A



minimum of 16k scans were accumulated at a spectral width of 250 kHz, and was Fourier transformed following 25 Hz exponential line broadening. 0° de-Paked spectra were obtained using an NMRPipe Macro [28].

### 2.3 Molecular dynamics (MD) simulations

The methodology of the simulations followed those implemented in [29]. In short, MD simulations utilised the GROMACS simulation suite version 5.0.2 [30-33]. The simulations were carried out at 310 K using a Nose-Hoover thermostat with a coupling constant of 0.5 ps. The pressure was maintained semi-isotropically at 1 bar using the Parrinello–Rahman barostat [34] with a relaxation time of 5.0 ps and a compressibility of  $4.5 \times 10^{-5} \text{ bar}^{-1}$ . A Lennard-Jones potential switch function was applied from 8 to 12 Å, and electrostatic interactions were treated using particle mesh Ewald [35, 36] with a real space cutoff of 12 Å. Neighbour lists were updated every 5 steps within the radius of 12 Å. We used our own virtual-sites implementation of lipids [37] with the CHARMM36 force field for lipids [38], thus enabling a time-step of 5 fs. All bonds were constrained by LINCS [39]. The simulations were run for 500 ns each.

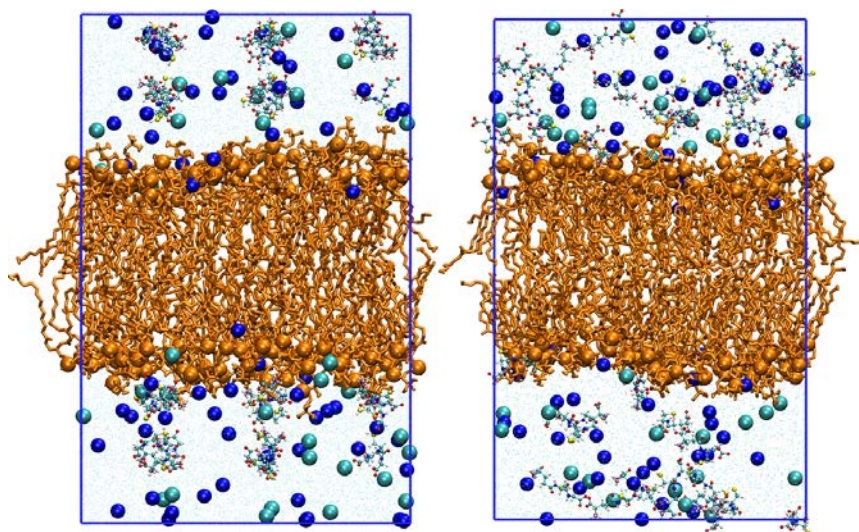


Figure 3: Initial (left) and final (right) snapshots from the simulations. The lipids are shown in orange, ions as spheres and the GSH molecules are shown in CPK representation. The phosphorus atoms of the lipids are shown as orange spheres. The water molecules which were explicitly included in the simulations have been omitted in the figure for the purposes of clarity.

The simulated systems were a 128-lipid pure DMPC bilayer, fully hydrated by 7580 water molecules, with an ionic NaCl concentration of 150 mM, and a second system containing the same bilayer with 32 GSH molecules initially placed randomly in the aqueous phase (see Fig. 3). The size of the simulation box was 6.1 x 6.1 x 9.9 nm. The total number of atoms in the simulation was 40,440.

#### *2.4 Glutathionylation of the Na<sup>+</sup>,K<sup>+</sup>-ATPase*

Solutions were designed to stabilise the enzyme in a particular conformational state, although fluctuations to other states cannot be excluded. Solutions stabilising the enzyme in an E1 conformation contained 100 mM NaCl. Solutions stabilising the enzyme in an E2 conformation contained either 100 mM KCl or 4 mM MgCl<sub>2</sub> together with 4 mM NaF. In addition, each solution contained 50 mM Tris and 1 mM EDTA, and the pH was titrated to a value of 7.2 with HCl. 1 mM of reduced GSH was added to either the E1 or E2 solutions and the pH was readjusted to 7.2 with NaOH (for the E1 solution) or KOH (for the E2 solutions). The enzyme was incubated in these solutions for 15 min at room temperature prior to immunoblotting. To measure alterations to  $\beta_1$  subunit glutathionylation we used SDS-PAGE followed by probing with anti-GSH antibody, as described previously [14, 40]. The intensity of chemiluminescence generated by the anti-mouse horseradish peroxidase secondary antibody used for the detection and amplification of the signal was quantified by

densitometric analysis (Fujifilm, LAS-3000). To verify comparable protein loading across experiments we also probed with an anti- $\beta_1$  antibody.

### **3. Results**

#### *3.1 Effect of glutathione on the di-8-ANEPPS fluorescence excitation ratio*

Fluorescence excitation spectra were recorded of di-8-ANEPPS bound to DMPC vesicles in the presence and absence of glutathione. Up to a glutathione concentration of 30 mM (the highest concentration studied) no observable shift in the excitation spectrum of the probe was detectable, i.e., there was no significant change in the value of the fluorescence excitation ratio,  $R$ , (see Materials and Methods) on the addition of glutathione. This is in contrast to a number of small inorganic anions, such as  $\text{ClO}_4^-$ ,  $\text{SCN}^-$ ,  $\text{I}^-$  and  $\text{NO}_3^-$ , which do cause significant shifts in the di-8-ANEPPS excitation spectrum [17]. For the most strongly binding anion found in that study,  $\text{ClO}_4^-$ , the intrinsic microscopic dissociation constant determined from the di-8-ANEPPS fluorescence excitation spectrum shift was  $44 (\pm 4)$  mM, i.e., similar to the highest concentration of glutathione used in this study. Thus, there is no evidence from the fluorescence measurements that glutathione is able to penetrate into a phosphatidylcholine bilayer, at least up to a glutathione concentration of 30 mM.

#### *3.2 Effect of glutathione on the NMR spectrum of phosphatidylcholine vesicles*

##### *3.2.1 Interaction with headgroup - $^{31}\text{P}$ NMR*

At 30°C, the  $^{31}\text{P}$  static NMR spectrum of glutathione-free d54-DMPC multilamellar vesicles (MLVs) showed a typical axially symmetric powder pattern of lipid bilayers in a fluid phase [41]. At 20:1 molar ratio of lipid to glutathione only a slight line sharpening of the  $^{31}\text{P}$  static spectrum was observed without change in the overall width (see Fig. 4, left panel). The MEMAS analysis of the  $^{31}\text{P}$  MAS experiments collected at 700 Hz, 900 Hz and 1200 Hz

spinning speed confirmed a similar CSA and asymmetry of about 31.5 ppm and 0, respectively, for both systems (see Fig. 4, right panel).

Relaxation measurements showed no significant effect of glutathione, with very similar  $T_1$  relaxation values of 0.607 s and 0.603 s for MLV without and with glutathione, respectively, indicating no perturbations of motions at the ns timescale such as lipid long axis rotation [42]. There was a small increase in  $T_2$  relaxation time in the presence of glutathione, from 11.0 ms to 12.8 ms, indicating some change in motions at the ms timescale such as membrane surface oscillation, which is consistent with the sharper  $^{31}\text{P}$  static spectrum (see Fig. S1).

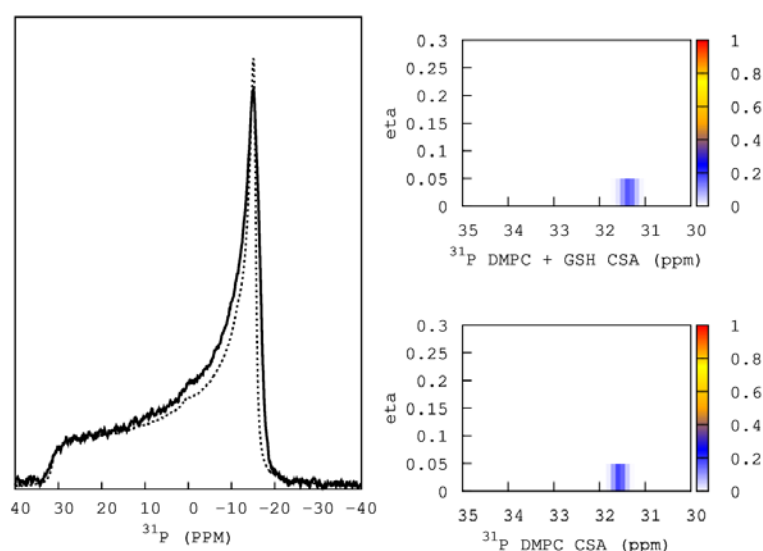


Figure 4: Left panel:  $^{31}\text{P}$  static NMR spectra of d54-DMPC multilamellar vesicles (solid line) and with a lipid to glutathione molar ratio of 20:1 (dotted line) with signal intensity plotted against chemical shift. Right panel: MEMAS analysis of  $^{31}\text{P}$  MAS experiments performed at three spinning speeds showing the chemical shift anisotropy and asymmetry (*eta*) in terms of population (colour scale).

### 3.2.2 Interaction with membrane hydrophobic core: $^2\text{H}$ NMR

At 30°C, the  $^2\text{H}$  static NMR spectrum of acyl chain deuterated DMPC MLVs displayed the typical quadrupolar splitting pattern of lipid bilayers in the fluid phase [42]. As was observed for the  $^{31}\text{P}$  static spectrum, the presence of glutathione at a lipid to glutathione molar ratio of 20:1 only induced a slight sharpening of the  $^2\text{H}$  spectrum but without change in the splittings (see Fig. 5). This indicates that glutathione does not penetrate into the lipid bilayer hydrophobic core but only slightly modifies the overall membrane slow motions.

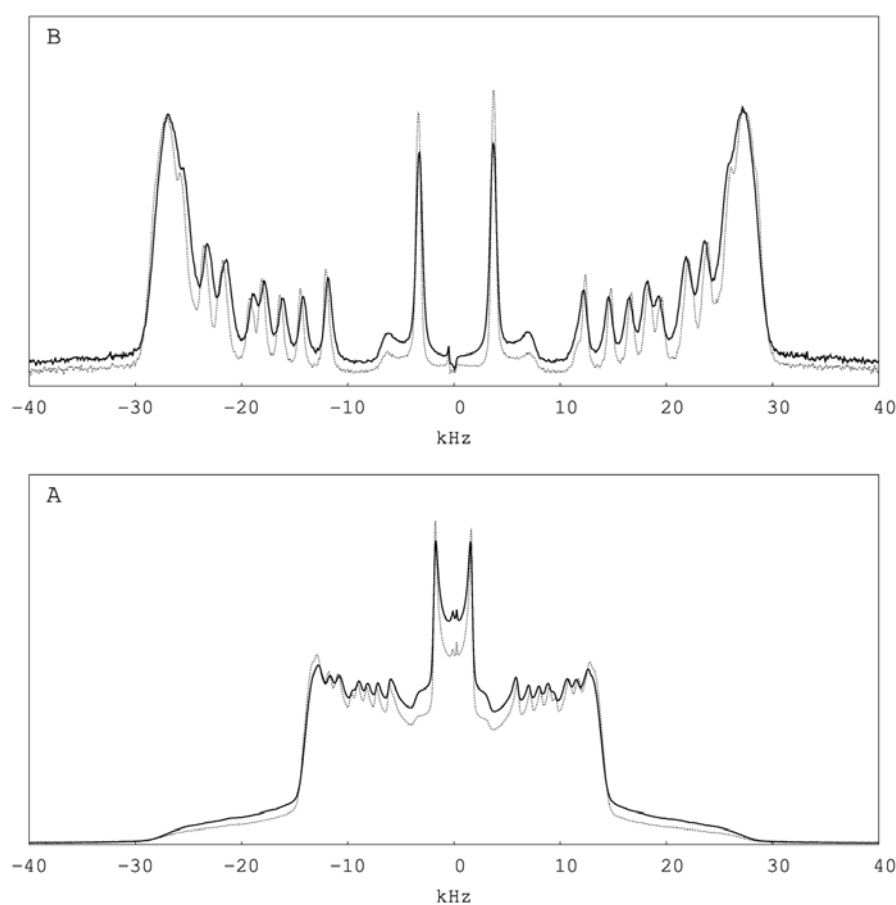


Figure 5: Top panel:  $^2\text{H}$  static NMR spectrum of d54-DMPC MLVs (solid line) and at a lipid to glutathione molar ratio of 20:1 (dotted line). Bottom panel: De-Paked spectra showing resolved quadrupolar splittings at a  $0^\circ$  orientation.

### 3.3 Molecular dynamics simulations of glutathione in the presence of DMPC membranes

Although the simulations predict that individual GSH molecules may visit the bilayer interface intermittently, the residence times of bound GSH molecules are not expected to exceed 100 ns (Fig. S2), indicating that GSH binding to the interface is likely to be transient (see Fig. 6). The average density maps along the bilayer normal also indicate that GSH molecules would be expected to prefer to localize at  $\sim 3$  nm from the bilayer centre, or, in other words, in the aqueous solution adjacent to the membrane, approximately 1 nm from the membrane/solution interface. Such trends are typical for hydrophilic charged molecules such as glutamate and GABA [43]. According to the simulations, the binding of GSH to the lipid interface is driven by electrostatic interactions. We quantify the specific interactions between GSH and the lipids by constructing the radial distribution function: a histogram of the instantaneous distances between specific chemical moieties over the entire production period of the simulation. The two carboxylate groups bind the positively charged choline group on the lipids, as indicated by peaks of the radial distribution functions at  $\sim 4$  Å, while the protonated N-terminus of the peptide binds strongly to the phosphate on the lipids, as indicated by the multiple sharp peaks at 3Å and 5Å in the radial distribution functions (see Fig. 7). In general, the carboxylate groups of GSH sit deeper in the bilayer than the N-terminus (data not shown). The simulations also predict that the bilayer thickness, area per lipid and the lipid tail orientational order parameters of DMPC are expected to be nearly unaffected by the presence of GSH (data not shown), in agreement with the NMR data.

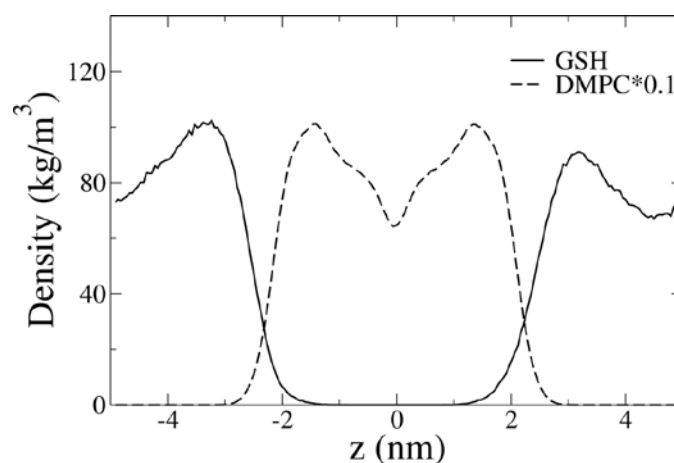


Figure 6: Average density of glutathione and DMPC lipids along the bilayer normal. The density of DMPC is scaled by a factor of 0.1 for visual aid. The peak at 3 nm from the bilayer centre is typical for charged hydrophilic molecules [43].

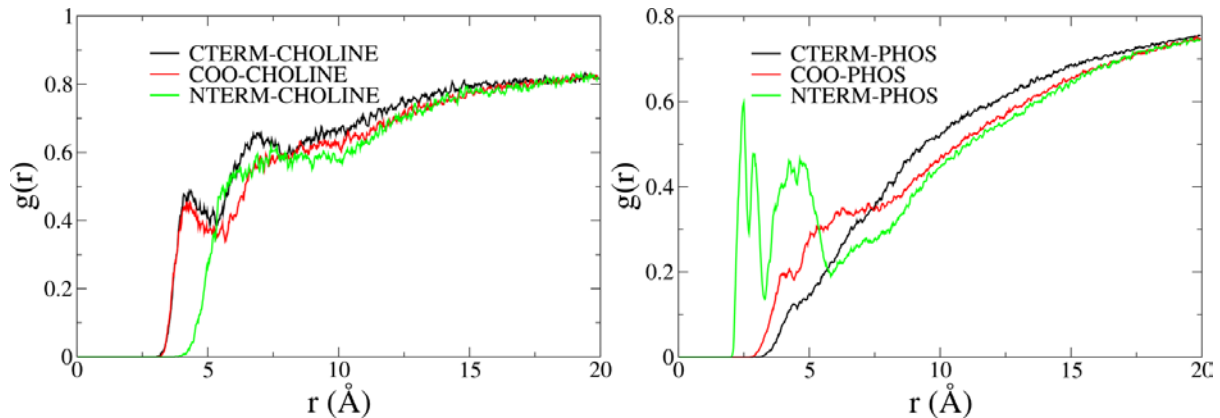


Figure 7: Radial distribution functions between the choline (left) and phosphate (right) moieties of DMPC and the charged N-terminus, C-terminus, and the glutamate carboxylate groups (COO) of GSH.

### 3.4 Glutathionylation of the $\beta_1$ -subunit of the $\text{Na}^+, \text{K}^+$ -ATPase

Immunoblots characterizing the level of glutathionylation of the  $\beta_1$  subunit of the  $\text{Na}^+, \text{K}^+$ -ATPase are shown in the upper portion of Fig. 8. In the lower part of the same figure the intensities of blots, quantified via densitometric analysis, are presented in a histogram format. There it can be seen that significant increases in  $\beta_1$  subunit glutathionylation are observed when the enzyme is incubated with 1 mM reduced glutathione in the E1 and E2 solutions. Furthermore, the apparent level of  $\beta_1$  subunit glutathionylation seems to favour the E1 conformational state over the E2 conformational state ( $P < 0.05$ ). This result implies that glutathione has easier access to cysteine residue 45 of the  $\beta_1$  subunit of the  $\text{Na}^+, \text{K}^+$ -ATPase when the enzyme is in an E1 conformational state.

This result is in agreement with a previous study [44], but there the level of glutathionylation was measured in the presence of the oxidant peroxynitrite. The results here indicate that oxidative damage to the  $\text{Na}^+, \text{K}^+$ -ATPase is not required for it to undergo glutathionylation of its  $\beta_1$  subunit.

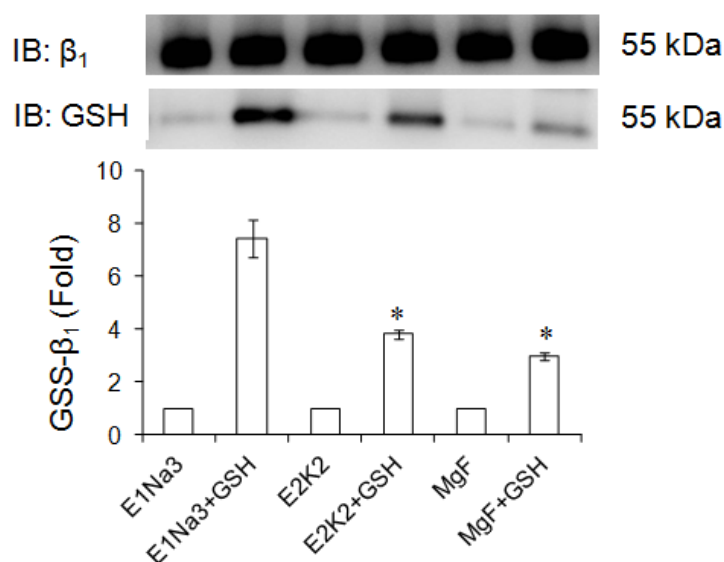


Figure 8: Glutathionylation level of the  $\beta_1$  subunit of the  $\text{Na}^+, \text{K}^+$ -ATPase in the E1Na<sup>+</sup><sub>3</sub>, E2K<sup>+</sup><sub>2</sub> and an E2-Pi-like (MgF<sub>4</sub><sup>2-</sup> stabilized) conformational states with and without 1 mM GSH. Glutathionylation was measured with the GSH antibody technique (see Materials and Methods). Immunoblots (IB) for the  $\beta_1$  subunit of the  $\text{Na}^+, \text{K}^+$ -ATPase and for enzyme-bound glutathione are shown above. The histogram shown displays the mean relative chemiluminescent intensity (expressed as Fold relative to the intensity before addition of glutathione)  $\pm$  S.E. of five experiments. \*,  $p < 0.05$  versus the E1Na3+GSH level.

#### 4. Discussion

The results of the fluorescence and NMR experiments reported here and the MD simulations carried out provide no support for the idea that glutathione is able penetrate at all into a phosphatidylcholine bilayer. At the physiological cytoplasmic glutathione



concentration of 5-10 mM the experimental and theoretical results obtained suggest that interaction of glutathione with the surface of the membrane is all one would expect.

In contrast, the experiments carried out using purified Na<sup>+</sup>,K<sup>+</sup>-ATPase-containing membrane fragments clearly show that cysteine residue 45 on the  $\beta$ -subunit of the protein can be glutathionylated, and that the degree of glutathionylation is significantly different depending on whether the protein is in the Na<sup>+</sup>-stabilized E1 or the K<sup>+</sup>-stabilized E2 state. This is despite the fact that, based on published crystal structures of the Na<sup>+</sup>,K<sup>+</sup>-ATPase [7-11], the cysteine residue is located in the transmembrane helix of the  $\beta$ -subunit. However, recent fluorescence data suggest that ion occlusion is accompanied by a significant conformational change which deforms the surrounding membrane [45]. In principle, a protein conformational change must indeed accompany ion occlusion to account for the fact that the transported ions have no access to either the cytoplasmic or the extracellular medium in the occluded state. Crystal structures of the Na<sup>+</sup>,K<sup>+</sup>-ATPase without occluded ions but with bound cardiotonic steroids [12, 13] show no significant displacement of Cys45 relative to the membrane surface in comparison to ion-occluded structures [7-11], indicating that the accessibility of Cys45 is most likely not due to a major displacement of the  $\beta_1$ -subunit towards the cytoplasm. This leaves, however, the possibility that the location of Cys45 relative to the  $\alpha$ -subunit could be significantly different in occluded and non-occluded protein states.

It seems, therefore, that these results can be reconciled only if the  $\beta$ -subunit of the Na<sup>+</sup>,K<sup>+</sup>-ATPase is not firmly attached to the  $\alpha$ -subunit, at least during some steps of the reaction cycle. Therefore in line with the idea, as also suggested by Thøgersen and Nissen [46], we propose that dissociation of the  $\beta$ -subunit from the  $\alpha$ -subunit by a slight twist or tilt could create a hydrophilic passageway between the two subunits allowing glutathione to access the cysteine residue from the cytoplasmic medium. As can be seen from Fig. 2, this

pathway is lined with polar residues, so that no major energetic barrier would be expected towards glutathione movement from the cytoplasmic medium to the site of the cysteine residue. In fact Liu et al. [44] already suggested a glutathione-induced dissociation of the  $\alpha$ - and  $\beta$ -subunits based on immunoprecipitation studies, which showed an inverse correlation between the co-immunoprecipitation of  $\alpha$ - and  $\beta$ -subunits of the  $\text{Na}^+, \text{K}^+$ -ATPase and the level of glutathionylation of the  $\beta_1$  subunit. Furthermore, there is experimental evidence based on voltage-clamp fluorometry [47] that the  $\beta$ -subunit does move slightly relative to the catalytic  $\alpha$ -subunit during the protein's reaction cycle, thus providing support for the latter of these scenarios for glutathione access. If the degree of interaction between the  $\alpha$ - and  $\beta$ -subunits alters as the protein undergoes the conformational changes necessary for ion pumping, this could explain the dependence of glutathionylation on enzyme conformational state reported here.

Finally, if, as the results presented here strongly suggest, glutathione is unable to enter the lipid membrane, once the  $\beta$ -subunit of the  $\text{Na}^+, \text{K}^+$ -ATPase becomes glutathionylated, this could anchor the cysteine in a hydrophilic environment, i.e., within a hydrophilic invagination of the membrane between the  $\alpha$ - and  $\beta$ - subunits, and hence inhibit motions of the  $\beta$ -subunit necessary for enzymatic activity. Thus, this would explain the strongly inhibitory effect of glutathionylation experimentally observed [6, 14]. The specific role of glutathionylation of Cys45 in the  $\beta_1$  subunit in the inhibition is indicated by a decrease in  $\text{Na}^+, \text{K}^+$ -ATPase activity induced by oxidant stress being eliminated by a Cys45  $\rightarrow$ Trp45 mutation of the  $\beta_1$  subunit expressed in *Xenopus* oocytes or by expression of  $\beta_2$  or  $\beta_3$  subunits that have no free Cys residue corresponding to Cys 45 of the  $\beta_1$  subunit [14]. The results presented here thus provide a possible mechanism whereby glutathionylation/deglutathionylation switches  $\text{Na}^+, \text{K}^+$ -ATPase activity off and on and hence

provide regulatory control over its function. This is supported by studies on cardiac myocytes (see below).

Exposure of isolated cardiac myocytes to the chemical oxidant paraquat induces glutathionylation of the Na<sup>+</sup>,K<sup>+</sup>-ATPase β<sub>1</sub> subunit and inhibits electrogenic Na<sup>+</sup>,K<sup>+</sup> pump current measured in voltage clamped cardiac myocytes. The inhibition is abolished by glutaredoxin 1 [14] that selectively reverses protein glutathionylation. Receptor-coupled Na<sup>+</sup>,K<sup>+</sup> pump regulation in cardiac myocytes can also be accounted for by glutathionylation of the β<sub>1</sub> subunit with increases and decreases in glutathionylation from baseline causing inhibition and stimulation, respectively. NADPH oxidase plays a central role in this regulation [48]. A similar scheme can account for Na<sup>+</sup>,K<sup>+</sup> pump inhibition induced by hyperglycemia *in vivo* and its reversal by treatment with a receptor agonist [49], indicating the pathophysiological and therapeutic relevance on glutathionylation-dependent pump regulation.

## **ACKNOWLEDGEMENT**

H.H.R. acknowledges, with gratitude, financial support (Project Grant 633252) from the National Health and Medical Research Council (Australia). R.J.C. received financial support from the Australian Research Council (Discovery Grants DP-121003548 and DP-150101112).

## REFERENCES

- [1] A. Pastore, G. Federici, E. Bertini, F. Piemonte, Analysis of glutathione: implication in redox and detoxification, *Clin. Chim. Acta* 333 (2003) 19-39.
- [2] G. Fiolomeni, G. Rotilio, M. R. Cirolò, Cell signalling and the glutathione redox system, *Biochem. Pharmacol.* 64 (2002) 1057-1064.
- [3] B. G. Hill, A. Bhatnagar, Protein S-glutathionylation: Redox-sensitive regulation of protein function, *J. Mol. Cell Cardiol.* 52 (2012) 559-567.
- [4] A. P. Fernandes, A. Holmgren, Glutaredoxins: Glutathione-dependent redox enzymes with functions far beyond a simple thioredoxin backup system, *Antioxidants and Redox Signaling* 6 (2004) 63-74.
- [5] T. Adachi, R. M. Weisbrod, D. R. Pimental, J. Ying, V. S. Sharov, C. Schöneich, R. A. Cohen, S-Glutathionylation by peroxynitrite activates SERCA during arterial relaxation by nitric oxide, *Nat. Med.* 10 (2004) 1200-1207.
- [6] H. H. Rasmussen, E. J. Hamilton, C.-C. Liu, G. A. Figtree, Reversible oxidative modification: Implications for cardiovascular physiology and pathophysiology, *Trends Cardiovasc. Med.* 20 (2010) 85-90.
- [7] J. B. Morth, B. P. Pedersen, M. S. Toustrup-Jensen, T. L.-M. Sørensen, J. Petersen, J. P. Andersen, B. Vilsen, P. Nissen, Crystal structure of the sodium-potassium pump, *Nature* 450 (2007) 1043-1049.
- [8] T. Shinoda, H. Ogawa, F. Cornelius, C. Toyoshima, Crystal structure of the sodium-potassium pump at 2.4 Å resolution, *Nature* 459 (2009) 446-450.
- [9] H. Ogawa, T. Shinoda, F. Cornelius, C. Toyoshima, Crystal structure of the sodium-potassium pump ( $\text{Na}^+, \text{K}^+$ -ATPase) with bound potassium and ouabain, *Proc. Natl. Acad. Sci. U.S.A.* 106 (2009) 13742-13747.
- [10] R. Kanai, H. Ogawa, B. Vilsen, F. Cornelius, C. Toyoshima, Crystal structure of a  $\text{Na}^+$ -bound  $\text{Na}^+, \text{K}^+$ -ATPase preceding the E1P state, *Nature* 502 (2013) 201-206.
- [11] M. Nyblom, H. Poulsen, P. Gourdon, L. Reinhard, M. Andersson, E. Lindahl, N. Fedosova, P. Nissen, Crystal structure of  $\text{Na}^+, \text{K}^+$ -ATPase in the  $\text{Na}^+$ -bound state, *Science* 342 (2013) 123-127.
- [12] M. Laursen, L. Yatime, P. Nissen, N. U. Fedosova, Crystal structure of the high-affinity  $\text{Na}^+, \text{K}^+$ -ATPase-ouabain complex with  $\text{Mg}^{2+}$  bound in the cation binding site, *Proc. Natl. Acad. Sci. U.S.A.* 110 (2013) 10958-10963.
- [13] M. Laursen, J. L. Gregersen, L. Yatime, P. Nissen, N. U. Fedosova, Structures and characterization of digoxin- and bufalin-bound  $\text{Na}^+, \text{K}^+$ -ATPase compared with the ouabain-bound complex, *Proc. Natl. Acad. Sci. U.S.A.* 112 (2015) 1755-1760.
- [14] G. A. Figtree, C.-C. Liu, S. Bibert, E. J. Hamilton, A. Garcia, C. N. White, K. K. Chia, F. Cornelius, K. Geering, H. H. Rasmussen, Reversible oxidative modification: a key mechanism of  $\text{Na}^+ - \text{K}^+$  pump regulation, *Circ. Res.* 105 (2009) 185-193.
- [15] S. A. Tatulian, Effect of lipid phase transition on the binding of anions to dimyristoylphosphatidylcholine liposomes, *Biochim. Biophys. Acta* 736 (1983) 189-195.
- [16] S. A. Tatulian, Binding of alkaline-earth metal cations and some anions to phosphatidylcholine liposomes, *Eur. J. Biochem.* 170 (1987) 413-420.
- [17] R. J. Clarke, C. Lüpfer, Influence of anions and cations on the dipole potential of phosphatidylcholine vesicles: A basis for the Hofmeister effect, *Biophys. J.* 76 (1999) 2614-2624.
- [18] I. Klodos, M. Esmann, R. L. Post, Large-scale preparation of sodium-potassium ATPase from kidney outer medulla, *Kidney Int.* 62 (2002) 2097-2100.

- [19] P. Ottolenghi, The reversible delipidation of a solubilized sodium-plus-potassium ion-dependent adenosine triphosphatase from the salt gland of the spiny dogfish, *Biochem. J.* 151 (1975) 61-66.
- [20] G. L. Peterson, A simplification of the protein assay method of Lowry et al. which is more generally applicable, *Anal. Biochem.* 83 (1977) 346-356.
- [21] O. H. Lowry, N. J. Rosebrough, A. L. Farr, R. J. Randall, Protein measurement with the Folin phenol reagent, *J. Biol. Chem.* 193 (1951) 265-275.
- [22] A. Zouni, R. J. Clarke, A. J. W. G. Visser, N. V. Visser, J. F. Holzwarth, Static and dynamic studies of the potential-sensitive membrane probe RH421 in dimyristoylphosphatidylcholine vesicles, *Biochim. Biophys. Acta* 1153 (1993) 203-212.
- [23] A. Zouni, R. J. Clarke, J. F. Holzwarth, Kinetics of solubilisation of styryl dye aggregates by lipid vesicles, *J. Phys. Chem.* 98 (1994) 1732-1738.
- [24] R. J. Clarke, D. J. Kane, Optical detection of membrane dipole potential: avoidance of fluidity and dye-induced effects, *Biochim. Biophys. Acta* 1323 (1997) 223-239.
- [25] R. J. Clarke, Effect of lipid structure on the dipole potential of phosphatidylcholine bilayers, *Biochim. Biophys. Acta* 1327 (1997) 269-278.
- [26] G. Cevc, Thermodynamic parameters of phospholipids, in: *Phospholipids Handbook*, G. Cevc (Ed.), Marcel Dekker Inc., New York, 1993, pp. 939-956.
- [27] M. A. Sani, F. Separovic, J. D. Gehman, Disentanglement of heterogeneous dynamics in mixed lipid systems, *Biophys. J.* 100 (2011) L40-L42.
- [28] M. A. Sani, D. K. Weber, F. Delaglio, F. Separovic, J. D. Gehman, A practical implementation of de-Pake-ing via weighted Fourier transformation, *PeerJ* 1(2013) e30.
- [29] V. V. Chaban, M. B. Nielsen, W. Kopec, H. Khandelia, Insights into the role of cyclic ladderane lipids in bacteria from computer simulations, *Chem. Phys. Lipids* 181 (2014) 76-82.
- [30] D. van der Spoel, E. Lindahl, B. Hess, G. Groenhof, A. E. Mark, H. J. C. Berendsen, GROMACS: Fast, flexible, and free, *J. Comput. Chem.* 26 (2005) 1701-1718.
- [31] H. J. C. Berendsen, D. van der Spoel, R. van Drunen, GROMACS: A message-passing parallel molecular dynamics implementation, *Comput. Phys. Commun.* 91 (1995) 43-56.
- [32] B. Hess, C. Kutzner, D. van der Spoel, E. Lindahl, GROMACS 4: Algorithms for highly efficient, load-balanced, and scalable molecular simulation, *Journal of Chemical Theory and Computation* 4 (2008) 435-447.
- [33] E. Lindahl, B. Hess, D. van der Spoel, GROMACS 3.0: a package for molecular simulation and trajectory analysis, *J. Mol. Model.* 7 (2001) 306-317.
- [34] M. Parrinello, A. Rahman, Polymorphic transitions in single crystals: A new molecular dynamics method, *J. Appl. Phys.* 52 (1981) 7182-7190.
- [35] U. Essmann, L. Perera, M.L. Berkowitz, T. Darden, H. Lee, L.G. Pedersen, A smooth particle mesh Ewald method, *J. Chem. Phys.* 103 (1995) 8577-8593.
- [36] T. Darden, D. York, L. Pedersen, Particle mesh Ewald: an N.log(N) method for Ewald sums in large systems, *J. Chem. Phys.* 98 (1993) 10089-10092.
- [37] B. Loubet, W. Kopec, H. Khandelia, Accelerating all-atom MD simulations of lipids using a modified virtual-sites technique, *J. Chem. Theory Comput.* 10 (2014) 5690-5695.
- [38] J. B. Klauda, R. M. Venable, J. A. Freites, J. W. O'Connor, D. J. Tobias, C. Mondragon-Ramirez, I. Vorobyov, A. D. MacKerell, R. W. Pastor, Update of the CHARMM all-atom additive force field for lipids: Validation on six lipid types, *J. Phys. Chem. B* 114 (2010) 7830-7843.

- [39] B. Hess, P-LINCS: A parallel linear constraint solver for molecular simulation, *J. Chem. Theory Comput.* 4 (2008) 116-122.
- [40] S. Bibert, C.-C. Liu, G. A. Figtree, A. Garcia, E. J. Hamilton, F. M. Marassi, K. J. Sweadner, F. Cornelius, K. Geering, H. H. Rasmussen, FXYP proteins reverse inhibition of the Na<sup>+</sup>-K<sup>+</sup> pump mediated by glutathionylation of its  $\beta_1$  subunit, *J. Biol. Chem.* 286 (2011) 18562-18572.
- [41] R. Smith, B. A. Cornell, M. A. Keniry, F. Separovic, P-31 nuclear magnetic resonance studies of the association of basic proteins with multilayers of diacyl phosphatidylserine, *Biochim. Biophys. Acta.* 732 (1983) 492-498.
- [42] A. Drechsler, F. Separovic, Solid-state NMR structure determination, *IUBMB Life* 55 (2003) 515-523.
- [43] G. H. Peters, M. Werge, M. N. Elf-Lind, J. J. Madsen, G. F. Velardez, P. Westh, Interaction of neurotransmitters with a phospholipid bilayer: A molecular dynamics study, *Chem. Phys. Lipids* 184 (2014) 7-17.
- [44] C.-C. Liu, A. Garcia, Y. A. Mahmmoud, E. J. Hamilton, K. K. Galougahi, N. A. S. Fry, G. A. Figtree, F. Cornelius, R. J. Clarke, H. H. Rasmussen, Susceptibility of  $\beta_1$  Na<sup>+</sup>-K<sup>+</sup> pump subunit to glutathionylation and oxidative inhibition depends on conformational state of pump, *J. Biol. Chem.* 287 (2012) 12353-12364.
- [45] L. J. Mares, A. Garcia, H. H. Rasmussen, F. Cornelius, Y. A. Mahmmoud, J. R. Berlin, B. Lev, T. W. Allen, R. J. Clarke, Identification of electric-field dependent steps in the Na<sup>+</sup>,K<sup>+</sup>-pump cycle, *Biophys. J.* 107 (2014) 1352-1363.
- [46] L. Thøgersen, P. Nissen, Flexible P-type ATPases interacting with the membrane, *Curr. Opin. Struct. Biol.* 22 (2012) 491-499.
- [47] R. E. Dempski, T. Friedrich, E. Bamberg, The  $\beta$  subunit of the Na<sup>+</sup>/K<sup>+</sup>-ATPase follows the conformational state of the holoenzyme, *J. Gen. Physiol.* 125 (2005) 505-520.
- [48] K. K. M. Chia, C.-C. Liu, E. J. Hamilton, A. Garcia, N. A. Fry, W. Hannam, G. A. Figtree, H. H. Rasmussen, Stimulation of the cardiac myocyte Na<sup>+</sup>-K<sup>+</sup> pump due to reversal of its constitutive oxidative inhibition, *Am. J. Physiol. Cell Physiol.* (2015) in press.
- [49] K. Karimi Galougahi, C.-C. Liu, A. Garcia, N. A. Fry, E. J. Hamilton, G. A. Figtree, H. H. Rasmussen,  $\beta_3$  adrenoreceptor activation relieves oxidative inhibition of the cardiac Na<sup>+</sup>-K<sup>+</sup> pump in hyperglycemia induced by insulin blockade, *Am. J. Physiol. Cell Physiol.* (2015) in press.